P2.7 IDEALIZED NUMERICAL SIMULATION OF THE EVOLUTION OF TROPICAL CYCLONE ELECTRIFICATION, LIGHTNING, MICROPHYSICS, AND KINEMATICS AT LANDFALL

Alexandre O. Fierro*[1], Lance M. Leslie*[1], Edward R. Mansell*[2,3], Jerry M. Straka*[1]
[1]School of Meteorology, Univ. of Oklahoma, Norman, OK
[2]Cooperative Institute for Mesoscale Meteorological Studies, Univ. of Oklahoma, Norman, OK
[3]NOAA/ NSSL, Norman, OK

1. INTRODUCTION

Emphasis is placed on the importance of increasing our knowledge of the microphysical and electrical structure of Tropical cyclones (TC), as a significant and novel step towards reducing model forecast errors in track and intensity predictions.
Although many studies (e.g. Black and Hallett, 1999) showed that mature TCs tended to be weakly electrified, several observational studies stressed the importance of more systematic monitoring of lightning activity in the vicinity of the eyewall as the latter is often accompanied by a strengthening of the TC (e.g. Lyons et al. 1989; Molinari et al. 1994). Regions of relatively large lightning flash rates in the TC were also suggested to be well correlated with the distribution of convective precipitation (Molinari et al. 1999). This knowledge is extremely important at landfall, providing advance warnings for both potential flooding and severe weather. Nevertheless, little is known at present about the actual changes occurring within the hydrometeor field and microphysics of a hurricane during landfall (on either flat or mountainous terrain) and, in turn, how these changes influence the electrical activity and intensity fluctuations of TCs.

2. EXPERIMENTAL DESIGN

The simulations shown herein was carried out in a 600 km x 600 km x 21 km domain with horizontal resolution of $\Delta x=\Delta y=2000$ m (300 x 300 x 35 grid points) up to 24 hours ahead. A stretched vertical grid was also used to better resolve the flow in the boundary layer ($\Delta z=200$ m near the surface to $\Delta z=900$ m at and above 7 km AGL). The vortex and initial wind profile are initialized with a modified Rankine vortex having a radius of 250 km with maximum relative vertical vorticity of $5*10^{-4}$ s^{-1}. Hence, no preliminary artificial vortex spin-up is required. For this reason and because we are focusing on cloud microphysical processes in mature TCs, the Coriolis force was turned off. The surface pressure at sea level is set to 1011 mb everywhere across the domain and the sea surface temperature is set to 30℃ in order to enhance surface fluxes efficiency. To reduce computational costs, electrification was turned off as sensitivity tests are still needed to determine the appropriate initial conditions. For the same reason, land has not been yet incorporated, and a 3-ice Lin-Farley Orville (LFO) type microphysics scheme is used instead of the far more advanced 10-ice scheme of Straka and Mansell (2004).

Initial Conditions

The initial environmental conditions were based on the 00 UTC San Juan sounding of September 13th 2003 (Fig. 1), which is the approximate time that Hurricane Isabel passed 400 miles north of the island. At that time Isabel was rated as a Category 5 storm on the Saffir-Simpson scale.

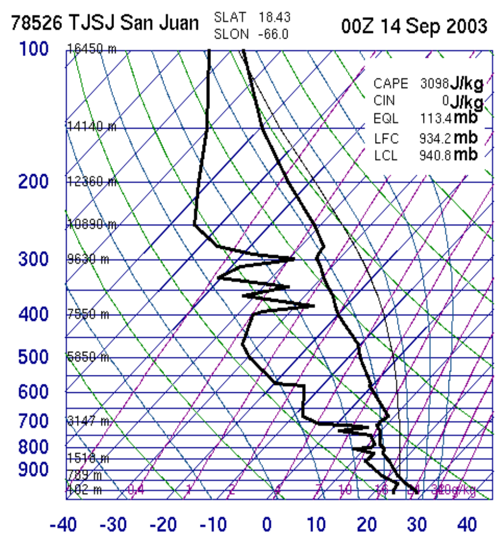

Fig. 1. a) 00 UTC San Juan Skew T–log p diagrams. of September 13th 2003. (Courtesy of the University of Wyoming).

Typical thermodynamic profiles in mature hurricanes are nearly moist adiabatic with low convective available potential energy (CAPE). In this study, effort is made in choosing a sounding representing the best the conditions in which TCs form and evolve, which is likely to be a more unstable environment. Additional simulations with lower CAPE soundings with low convective inhibition (CIN) are currently on their way.

3 RESULTS AND DISCUSSION

The main goal of this work was to determine qualitatively and quantitatively how the simulated TC microphysics and subsequent electrification evolves at landfall. Towards this goal, control simulations without land/orograpy were carried out and are shown below

Kinematic and microphysics evolution.

After 20 hours of simulation, the vortex has developed a distinct eyewall with a main connection rainband on its eastern flank. At this time, the minimum surface pressure is about 984 mb. Tangential winds exceed 40 m/s at sea level with higher gusts just above the boundary layer (Fig. 3a), corresponding to a high-end Category 1 storm. The horizontal reflectivity profile shown in Fig. 2a reveals structures typical of mature hurricanes, such as more continuous convection near the center, with discrete storm cells in the outer bands. Between these two convective regions, a stratiform region with weak reflectivity values is also evident (also see Fig 3b). After 24 hours, sporadic convection starts to develop rapidly in the southwest quadrant of the TC. This enhanced convective activity causes the storm circulation to weaken and the progressive TC demise. A possible but not exclusive explanation for this behavior might be the excessive amount of CAPE present in the sounding used as initial condition in the whole domain. Additionally, the lack of convective inhibition would also favor erratic secondary cell development throughout the domain.

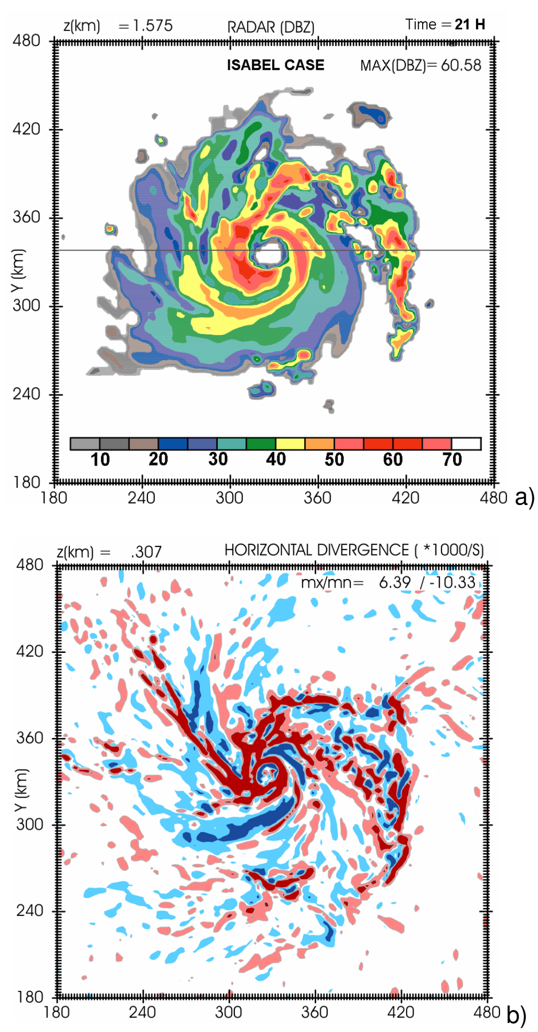

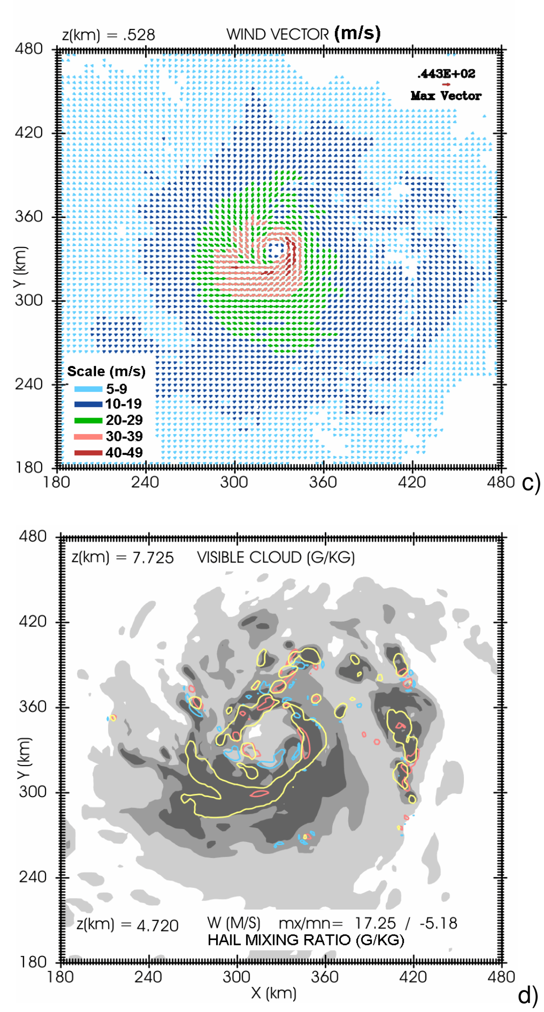

Fig. 2 a) Horizontal cross section of radar reflectivity (dBZ) at z=1.57 km shown by 5 dBZ contour increments from 5 dBZ to 75 dBZ. The thin gray line show the cross section location of the cross sections shown below in Fig. 2. Fig. b) shows the horizontal divergence field at 0.3 km, with convergence (divergence) shown in red (blue). Light (darker) blue and red contours depict regions where divergence magnitude exceeds 3.e-04 s-1 (1.e-3). Fig. c) shows the horizontal wind vector field magnitude at z=0.5 km. Finally, Fig. d) is a composite of hail mixing ratio (0.5 contour g/kg shown in yellow) and vertical wind at 4.7 km (blue contours showing regions where w ≤ -2m/s and red where w ≥ 5 m/s), and cloud mixing ratio at 7.7 km (with 0.1 g/kg filled contours in light gray, 0.5 g/kg in medium gray and 1 g/kg in darker gray).

The vertical cross sections through the eye in Figs. 3a and 3b show regions of persistent convection filled with graupel and small hail within the eyewall, which are collocated with the largest liquid water content values (Figs. 3a). As a result, sufficient charging might occur within confined regions of the eyewall, allowing lightning discharges to occur. Furthermore, Figs. 2d and 3a show that moderate hail/graupel mixing ratios (> 0.5 g/kg) are primarily found in the eyewall and in the individual convective cells forming the connecting rainbands. Consequently, charging able to produce lightning may also occur within the strongest cells in the outer rainbands. The heaviest rainfall amounts and hence larger reflectivity values are also found in the vicinity of the eyewall with a secondary maximum in the outer rainband (Figs. 2a and 3b).

The 0°C and –10°C isotherms rise in altitude inside the eye, which is consistent with hurricanes being warm cored lows. The lighter ice crystals and snow particles nucleating inside the eyewall are advected radially outward (Figs. 3a) to form a weak-echo stratiform region, commonly referred as the outer eyewall (Figs. 2a and 3b). Eventually, some of the larger crystals melt and start falling outside the eyewall precipitation core.

The outer eyewall southwest of the TC is coincident with regions dominated by horizontal divergence (Fig. 2b), which would tend to indicate that this region of the outer eyewall on the right side of the TC is a region dominated by weak downdrafts primarily composed of (melting) ice crystals and snow particles and aggregates. In contrast, the two regions dominated by updrafts, namely the eyewall and the main connecting rainband (Figs. 2a and 3a), are correlated in space with regions of horizontal convergence (Fig. 2b). The eyewall is coincident with areas of horizontal convergence (Fig. 2b), while the eye itself is mainly characterized by diverging winds likely attributed to descending motions.

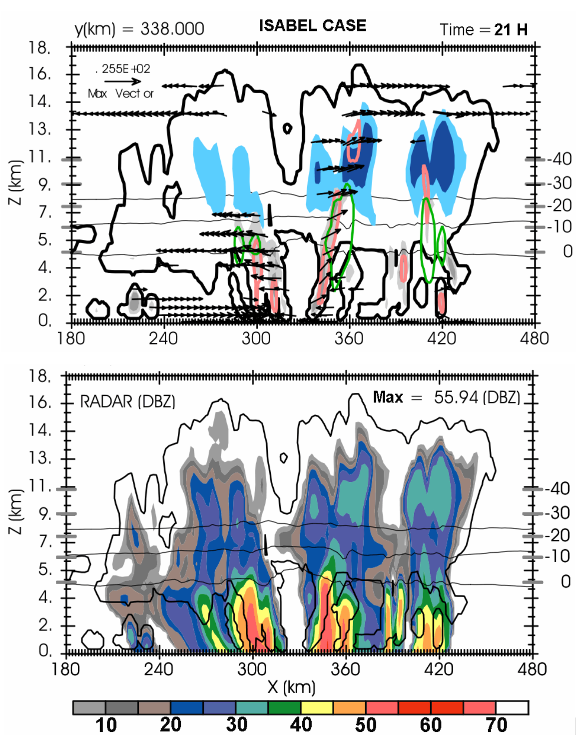

a)

b)

Fig. 3). In a) updraft speeds greater than 10 m/s are shown by the red contours. Liquid water contents (LWC) is also shown in shaded areas as follows: light grey for LWC ≥ 0.1 g/kg, medium grey for LWC ≥ 0.5 g/kg and darker gray for LWC ≥1 g/kg. Green contours depict regions of the storm where the hail mixing ratio exceeds 0.5 g/kg. Light (dark) blue-filled area shows snow mixing ratios greater than 0.5 (2.0) g/kg. Fig b shows a vertical cross section of radar reflectivity (dBZ) at 5 dBZ contour intervals from 10 dBZ to 70 dBZ through the eyewall(as shown by the thin grey horizontal line in Fig 2a). The black thick line depicts the cloud boundary shown by the 0.01 g/kg cloud mixing ratio.

4. FUTURE GOALS

At present, little is known about the actual changes occurring within the hydrometeor field and microphysics of a hurricane during landfall (on flat or mountainous terrain) and in turn how these changes influence the TC electrical activity and intensity fluctuations. Towards this goal, this work is intended to help answer questions such as:

- Does the simulated storm produce greater graupel/hail volume mass fluxes at low levels during landfall? If so, is the latter more pronounced within the rainbands or within the inner core region?
- How does the net charge density structure differ within the inner core and inside the rainbands? Does the middle level charge region experience a downslope/upslope trend as a TC makes landfall?
- Which of intra-cloud or cloud to ground lightning flash rates experience the most drastic changes and how is this related to changes observed in the hydrometeor field and intensity of the storm?

Higher resolution simulations will be performed on the new Itanium® high-performance supercomputer at the Oklahoma Supercomputing for Education and Research (OSCER) center in Norman, scheduled to be available by mid-December 2004. Furthermore, a Message Passing Interface (MPI) version of the model code will be provided to allow higher resolution simulations.

These numerical simulations will be performed on a 1200x1200x36 domain with horizontal resolution of 1 km, variable vertical resolution in the vertical and a lightning resolution of 500 m.

Acknowledgements: We thank the Organization of Naval Research (*ONR)* for generously sponsoring Alexandre Fierro (Grant N00014-02-1-0181); and The Oklahoma Supercomputing Center for Education and Research (*OSCER)* for providing the computing resources. Partial support for this research was also provided by the National Science foundation *(NSF)* under grants ATM-0119398 (E. Mansell) and ATM-0340693 (J. Straka)

REFERENCES

Black, R. A. and J. Hallett, 1999: Electrification of the hurricane, *J.Atmos Sci*, **56**, 2004-2028.

Lyons, W.A., M.G. Venne, P.G. Black and R.C. Gentry, 1989: Hurricane lightning: A new diagnostic tool for tropical storm forecasting? Preprints, 18th Conf. on Hurricanes and Tropical Meteorology, San Diego, American Meteorological Society, 2 pp.

Molinari, J., P.K. Moore, V.P. Idone, R.W. Henderson, and A.B. Saljoughy, 1994: Cloud-to-ground lightning in Hurricane Andrew. *J. Geophys. Res.*, **99**, 16665-16676.

Molinari, J., P. Moore, V. Idone, April 1999: Convective structure of hurricanes as revealed by lightning locations, *Mon. Wea. Rev.*, **127**, 520 - 534.

Straka, J. M. and E. R. Mansell, 2005: A bulk microphysics parameterization with multiple ice precipitation categories. Accepted in *J. Appl. Meteor.*